

SYNTHESIS AND MICROSTRUCTURE CHARACTERIZATION OF SOL-GEL DERIVED PHASE FRACTIONS IN PZT NANOPOWDERS

E. A. EID, M. R. EBIED, M. A. KAID, M. G. S. ALI*

Physics Department, Faculty of Science, Minia University, Minia 61519, Egypt

Lead zirconate titanate (PZT) nanopowders with the composition of $\text{Pb}(\text{Zr}_{0.52}\text{Ti}_{0.48})\text{O}_3$ were synthesized by a sol-gel process. The prepared PZT powders were calcinated at 500 °C, 600 °C, 700 °C and 750 °C for 1 h. Thermal, vibrational and Structural characteristic of PZT powder have been studied, using thermogravimetric analysis (TGA), fourier transform infrared (FTIR) spectroscope, and powder x-ray diffraction (XRD). Results showed that single phase perovskite pzt powders were obtained at temperature of 750 °C. By using materials analysis using diffraction (Maud) program the anisotropic microstructural characteristics (crystallite size and microstrain) and lattice parameters at different calcination temperature were determined, using anisotropic no rules approach. Also, from the same program weight fractions of tetragonal and rhombohedral phases in pzt powders at different calcination temperature were calculated.

(Received February 12, 2020; Accepted May 14, 2020)

Keywords: PZT nanopowders, Microstructural characteristics, Maud program, Weight fractions

1. Introduction

Lead zirconate titanate (PZT) in their perovskite structure is an interesting ferroelectric material. This material has good piezoelectric properties, relatively high Curie temperature, and relatively low sintering temperatures [1-2]. As a result of these properties, PZT material has become a suitable candidate for many applications, for example, sensors, computer memory, actuators, modulators etc. [3-4]. PZT powders have been synthesized by several methods. The sol-gel method has obtained special interest due to remarkable advantages comparing with other methods. Chontira Sangsubun [5] prepared pzt powder by a modified sol-gel processing method. The synthesized powder has tetragonal structure with a very small amount of pyrochlore phase at 700 °C. Guohong Mu and Mingyuan Gu [6] obtained uniform single phase PZT powders at calcination temperature of 700 °C for 2.5 h with average particle size 70 nm.

In this paper, we prepared single phase PZT nanopowders at calcination temperature of 750 °C for 1 h by sol-gel process. Also, we investigated the effect of calcination temperature on the formation of pzt phases, and calculated the weight fractions of multi-phases PZT powders.

2. Experimental details

The starting chemicals used for the preparation of PZT precursor were lead acetate ($\text{Pb}(\text{CH}_3\text{COO})_2 \cdot 3\text{H}_2\text{O}$, 99.5% Merck), Zirconium n-propoxide ($\text{Zr}(\text{OCH}_2\text{CH}_2\text{CH}_3)_4$, 70% in propanol, Sigma-Aldrich), Titanium isopropoxide ($\text{Ti}(\text{C}_3\text{H}_7\text{O})_2$, 98% Merck), and 2-methoxyethanol ($\text{C}_3\text{H}_7\text{OOH}$, 99.3% Merck).

Firstly, 5.23 g lead acetate was dissolved in 20 ml 2-methoxyethanol and stirred at room temperature for 1 h. Secondly, 5.927 g of titanium isopropoxide and 10.571 g of zirconium propoxide were added to 10 ml of 2-methoxyethanol the solution then stirred for 30 min. Finally, lead solution was added to zirconium-titanium solution, and stirring was continuously carried out

* Corresponding author: mgalal09@yahoo.com

for 30 min at 60 °C temperature. The gel was dried at 60 °C for 2 days. Then the dried gel was milled and calcinated at 500°C, 600°C and 700°C, and 750 for 1 h.

3. Results and discussion

3.1. Thermal analysis (TGA)

The thermal behavior of dried gel of PZT was characterized, using thermogravimetric analysis (TGA). TGA was carried out on PZT gel powder dried at 60 °C at a heating rate of 20 C min⁻¹. Fig. 1 illustrates the results of (TGA) analysis. The TGA curve reveals three main regions in the range of 34-600°C. The weight loss in the first region from 34-100°C is due to removal of remnant water. The second region present between 100–500 °C. In this part the weight loss is due to the decomposition of light organics and acetates [7]. Finally, after 500°C no further weight loss or other chemical reactions were observed, which reflect the crystallization of PZT powder [8].

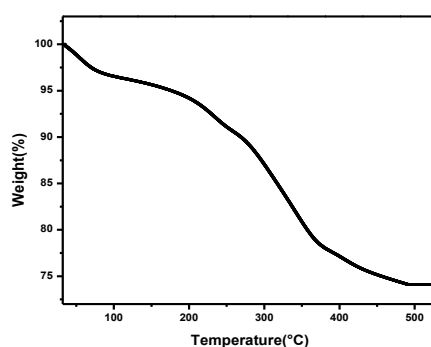


Fig. 1. Thermal analysis(TGA) of PZT dried gel.

3.2. FTIR analysis

The FTIR spectrum of the pzt powders calcinated for 1 h at different calcination temperatures were recorded in range of (400–3998) cm⁻¹ as shown in Fig. 2. In the spectrum the band at 597 cm⁻¹ is related to metal-o-metal bonds of the PZT phase [9]. The vibration band around 1401 cm⁻¹ is assigned to C-O bonds [10]. Additionally, the bands at 1584 cm⁻¹ and 1632 cm⁻¹ indicate the asymmetric stretching vibrations of carboxyl groups C=O [10]. Finally, the band observed at 3408 cm⁻¹ is resulted from the stretching vibration of the hydrogen bonded O-H groups [11].

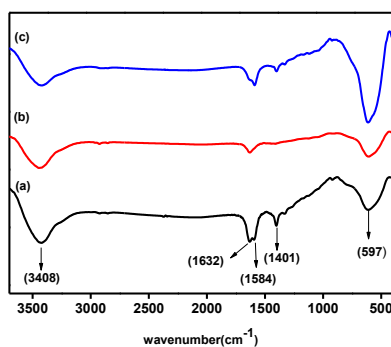


Fig. 2. FTIR spectra of prepared PZT powder at different calcination temperatures for 1hrs: 600 °C(a), 700 °C(b), 750 °C(c)

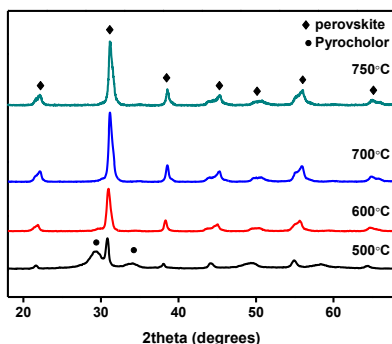


Fig. 3. XRD patterns of PZT powders calcinated at different temperatures

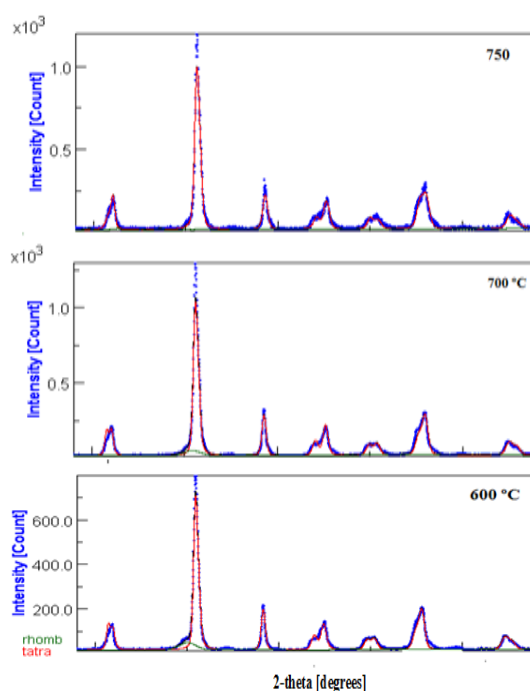


Fig. 4. Maud fit for PZT powders at 600 °C, 700 °C, and 750 °C

3.3. Structural analysis

Fig. 3 shows XRD patterns for the powders calcinated at 500°C, 600°C, 700°C, and 750°C for 1 h. X-rays data was collected from prepared PZT sample using PANalytical X'pert diffractometer. Data was collected within range of 18°-92° and step size 0.02 with the Cu-K α_1 radiation ($\lambda = 1.5406 \text{ \AA}$). For sample calcinated at 500 °C the figure reveal that pzt nanopowders were rhombohedral phases with some pyrochlore phase. It is observed from the XRD patterns of the sample calcinated at temperatures 600 °C that pyrochlore phase was completely removed, while mixture between rhombohedral and tetragonal phases is observed. By increasing the calcination temperature to 750 °C the single phase perovskite pzt powders with tetragonal crystal structure is obtained. The MAUD analysis of PZT diffraction data is depicted in figure 4. Good fit between refined and observed diffraction pattern (Fig. 5) was achieved with $R_w = 15.9, 18, 21.4$ for analysis at 600 °C, 700 °C, and 750 °C, respectively. Table 1 represents the lattice parameters and weight fractions of PZT powders calcinated at 600 °C, 700 °C, and 750 °C calculated by Maud program. At 600 °C PZT powders contain two phases rhombohedral and tetragonal phases the weight fractions of these two phases are 73 %, 27% respectively. By increasing temperature to 700 °C, the weight fraction of tetragonal increased to 91 %, and weight fraction of rhombohedral decreased to 9 %. Raising temperature to 750 °C tetragonal weight fraction reached to 98%, so the dominant

phase at 750°C is tetragonal. Table 2, Table 3, Table 4 show the anisotropic crystallite size and microstrain values determined by Maud program for PZT powders calcinated at different temperature.

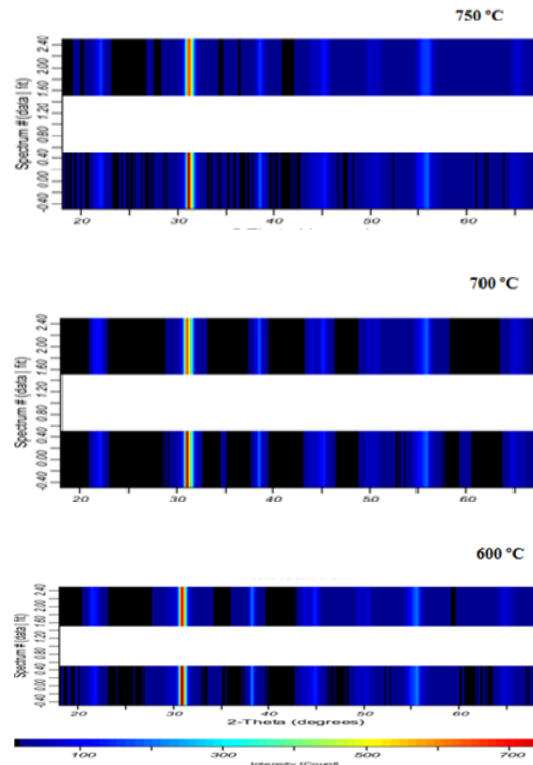


Fig. 5. 2D contour of PZT sample calcinated at 600 °C, 700 °C, and 750 °C.

Table 1. The lattice parameters and weight fractions of PZT powders calcinated at 600°C, 700°C, and 750 °C.

Temperature (°C)	Structure	Lattice parameters	weight fractions (%)
600	Rhombohedral	a=b=c=4.17 (Å) $\alpha = \beta = \gamma = 90.46$	27
	Tetragonal	a=b=4.02 (Å) c=4.11(Å) $\alpha = \beta = \gamma = 90$	73
700	Rhombohedral	a=b=c=4.09 (Å) $\alpha = \beta = \gamma = 89.95$	9
	Tetragonal	a=b=4.006(Å) c=4.099 (Å) $\alpha = \beta = \gamma = 90$	91
750	Rhombohedral	a=b=c=4.1 (Å) $\alpha = \beta = \gamma = 89.6$	2
	Tetragonal	a=b=3.99 (Å) c=4.08 (Å) $\alpha = \beta = \gamma = 90$	98

Table 2. Crystallite size and microstrain for pzt calcinated at 600 °C.

Rhombohedral			Tetragonal		
hkL	Crystallite size (nm)	Microstrain	h k L	Crystallite size (nm)	Microstrain
100	18.8	0.0357	0 0 1	75.9	0.0049
110	52.4	0.0253	110	29.7	0.0022
111	48.3	0.0686	111	50.1	0.0033
200	18.8	0.0357	200	27.4	0.0026
210	36.2	0.0391	102	69	0.0045
211	36.6	0.0547	112	46.3	0.0042
220	52.4	0.0352	202	57.1	0.0039
221	51.1	0.0446	220	29.7	0.0022
300	18.8	0.0357	212	54.0	0.0037
310	28.8	0.0339	103	72.5	0.0047

Table 3. Crystallite size and microstrain for pzt calcinated at 700 °C.

Rhombohedral			Tetragonal		
hkL	Crystallite size (nm)	Microstrain	hkl	Crystallite size (nm)	Microstrain
100	29.9	0.035	0 0 1	91.0	0.0052
110	39.1	0.024	110	35.1	0.0026
111	38.3	0.045	111	59.9	0.0037
200	29.9	0.035	200	35.9	0.0032
210	33.9	0.031	102	83.0	0.0049
211	34.3	0.040	112	77.0	0.0045
220	39.1	0.024	202	69.2	0.0043
221	38.8	0.033	220	35.1	0.0026
300	29.9	0.035	212	66.2	0.0041
310	32.0	0.033	103	87.1	0.0050

Table 4. Crystallite size and microstrain for pzt calcinated at 750 °C.

Rhombohedral			Tetragonal		
hkL	Crystallite size (nm)	Microstrain	hkl	Crystallite size (nm)	Microstrain
211	49.5	0.014	0 0 1	17.1	0.0008
222	50.1	0.019	110	51.6	0.0047
221	50.5	0.011	111	43.3	0.0039
210	49.6	0.0055	200	59.2	0.0056
200	48.9	0.006	102	30.6	0.0026
322	49.8	0.016	112	32.9	0.0028
220	50.7	0.0043	202	43.6	0.0040
310	49.3	0.0058	220	51.6	0.0047
300	48.9	0.006	212	43.5	0.0040
330	50.7	0.0043	103	24.8	0.0019

4. Conclusions

PZT powders with single and multi-phases were prepared by sol-gel process. FTIR, TGA and XRD analysis were used to characterize the synthesized powder. From recorded result the single phase pzt powder with tetragonal structure was obtained at 750 °C. The weight fractions of tetragonal and rhombohedral in prepared powder at different calcination temperature was calculated using Maud program. Also, lattice parameter, crystallite size, and microstrain were determined using the same program.

References

- [1] G. H. Haertling, J. of the American Ceramics Society **82**, 797 (1999).
- [2] A. J. Moulson, J. M. Herbert, Electroceramics, Chapman and Hall, London, 1999.
- [3] M. Nagao, K. Minami, M. Esashi, Sensor Materials **11**, 31 (1999).
- [4] K. Kim, Y. J. Song, Microelectronics Reliability **43**, 385 (2003).
- [5] S. Chontira, N. Manoch, W. Anucha, T. Tawee, J. Sukanda, J. Special Issue on Nanotechnology **4**, 53 (2005).
- [6] M. Guohong, Y. Shiyuan, L. Jufen, G. Mingyuan, J. materials processing technology **182**, 382 (2007).
- [7] Z. J. Xu, R. Q. Chu, G. R. Li, Xin Shao, Q. R. Yin, Materials Science and Engineering **117**, 113 (2005).
- [8] M. Prabu, I. B. Shameem Banu, S. Gobalakrishnan, M. Chavali, S. Umapathy, Advanced Science Engineering and Medicine **5**, 1 (2013).
- [9] R. Auer Zimmermann-Chopin, J. Sol-Gel Science and Technology **3**, 101 (1994).
- [10] A. Khorsand Zak, W. H. Abd. Majid, M. Darroudi, J. Optoelectron. Adv. M. **12**, 1714 (2010).
- [11] K. Uchino, Comprehensive Composite Materials, Elsevier, 523 (2000).